



Urban-rural patterns and driving factors of particulate matter pollution decrease in eastern china

Zhihao Song^{1, 2}, Bin Chen^{1, 2}

¹ College of Atmospheric Sciences, Lanzhou University, Lanzhou 730000, China

² Institute of Meteorological Artificial Intelligence Research, Lanzhou University, Lanzhou 730000, China

Correspondence to: Bin Chen (chenbin@lzu.edu.cn)

Abstract. Urban-rural patterns of particulate matter (PM) pollution reduction in China remain poorly understood. Using an interpretable end-to-end machine learning model framework from original satellite data, we identified changes in urban and rural PM pollution and the underlying drivers. During the period 2015-2023, the average decrease rates of PM₁₀ and PM_{2.5} in eastern China were $-4.1 \pm 1.1 \mu\text{g}/\text{m}^3/\text{month}$ and $-2.4 \pm 0.8 \mu\text{g}/\text{m}^3/\text{month}$, respectively. The rate of decrease in urban areas was higher than that in rural areas, which played a dominant role in PM reduction. Significant reductions in PM concentrations were observed in urban core areas, suburbs, towns and regions with high agricultural pressure. The interpretability analysis showed that temperature and interannual variability were the main drivers of PM pollution reduction. However, only interannual variability showed a significant decreasing trend in its effect on PM pollution, while other driving factors showed periodic variations. Furthermore, there were differences in the drivers of PM reduction between urban and rural areas, particularly with interannual variability in particular contributing to PM pollution reduction in urban areas, but having a lesser impact in most rural areas. This study reveals the urban-rural patterns of PM pollution reduction in eastern China, and highlights the need for differentiated air pollution control strategies in urban and rural areas.

1 Introduction

Air pollution caused by PM_{2.5} and PM₁₀ (airborne particulate matter with diameters less than 2.5 μm and 10 μm , respectively) has adversely affected China's atmospheric environment (Huang et al., 2014a; Zhang et al., 2012). PM pollution is now considered the greatest environmental risk factor for global human health (Apte et al., 2015), as exposure to PM can trigger various respiratory and cardiovascular diseases (Burnett Richard et al., 2014; West et al., 2016; Cohen et al., 2017). The indirect health risks associated with PM exposure (Yin et al., 2020) contribute to millions of premature deaths annually in



28 China (Burnett et al., 2018). To mitigate the escalating risks of particulate matter exposure and reduce
29 the public health burden, the Chinese government introduced the "Air Pollution Prevention and Control
30 Action Plan" in 2013 (State Council of the People's Republic of China, 2013). This initiative aims to
31 implement policies to improve energy efficiency, reduce energy-related pollution, and curb
32 anthropogenic emissions to control particulate matter pollution in the atmosphere (State Council of the
33 People's Republic of China, 2014). As a result of this initiative, China's atmospheric particulate matter
34 pollution has improved significantly (Cheng et al., 2021). Between 2013 and 2017, the annual average
35 concentration of PM_{2.5} decreased by 28-40% (Zheng et al., 2018; Ministry of Ecology and Environment
36 of the People's Republic of China, 2017), and the population-weighted national annual average
37 concentration of PM_{2.5} decreased by 32% (Xue et al., 2019). Data from the National Air Quality
38 Monitoring Network show that between 2013 and 2020, the annual average PM_{2.5} concentration in urban
39 areas of China decreased from 72 µg/m³ to 33 µg/m³ (Song et al., 2023). As a result, the Clean Air Action
40 has achieved remarkable results in reducing PM pollution (Zhang et al., 2019b).

41 It is widely accepted that improvements in air quality can be attributed to both reductions in
42 anthropogenic emissions (Geng et al., 2019; Zheng et al., 2023; Zhao et al., 2018) and changes in
43 meteorological conditions (An et al., 2019; Cao and Yin, 2020; Chen et al., 2020a). To assess the driving
44 factors behind changes in PM concentration trends, it is essential to distinguish between anthropogenic
45 emissions and meteorological factors (Zhong et al., 2018). Zhong et al. (2021) found that PM_{2.5}
46 concentrations decreased by 44% from 2013 to 2019, and by 34% when the influence of meteorological
47 conditions was excluded, thus demonstrating the effectiveness of emission reduction measures. Qiu et al.
48 (2022) used the GEOS-Chem chemical transport model to simulate the impact of anthropogenic
49 emissions on PM pollution trends and provided recommendations for attributing PM pollution trends to
50 emission changes. Vu et al. (2019) used machine learning to assess the impact of air quality trends in
51 Beijing and found that PM_{2.5} and PM₁₀ concentrations decreased by 34% and 24%, respectively, after
52 excluding meteorological influences, attributing the decrease to reduced coal burning. Zhai et al. (2019)
53 used a stepwise multiple linear regression (MLR) model to quantify PM_{2.5} trends in China between 2013
54 and 2018, and found that meteorological conditions contributed about 12%. However, Xiao et al. (2021)
55 used statistical methods to separate the contributions of emissions and meteorology to long-term PM_{2.5}
56 trends in East China, and found that meteorological contributions were even higher in certain years.



57 Overall, distinguishing the contributions of anthropogenic emissions and meteorological changes to PM
58 pollution is crucial to improve understanding of pollution processes and to inform pollution control
59 policies and future air quality predictions.

60 However, the urban-rural patterns of PM pollution improvement remain poorly understood in
61 existing research (Chen et al., 2020b). Many studies on PM pollution either focus on highly polluted
62 regions (such as the Beijing-Tianjin-Hebei region) (Chen et al., 2019a; Chen et al., 2019b), or on
63 developed regions with a high concentration of large cities (such as the Yangtze River Delta and the
64 Pearl River Delta) (Gui et al., 2019; He et al., 2017). This focus is mainly due to the high concentrations
65 of air pollutants in developed cities (Sicard et al., 2023), where PM pollution poses a significant public
66 health threat to densely populated urban areas (Brauer et al., 2016; Southerland et al., 2022). Although
67 PM pollution in urban areas highlights the importance of environmental governance, rural areas, with
68 different consumption habits and living conditions (e.g., solid fuel burning in households) (Li et al.,
69 2014)), may experience air pollution that differs from urban areas (Wang et al., 2024a). In certain seasons
70 and regions, PM exposure factors in rural areas are generally higher than those in urban areas, with
71 exposure levels reaching up to 70% (Wang et al., 2024b). Therefore, the contribution of these regions to
72 PM pollution improvement may differ (Li et al., 2024b). Without targeted assessments, perceptions of
73 the relative importance of urban and rural areas in China's air pollution control efforts may be distorted,
74 hindering the development of appropriate environmental policies and the promotion of green
75 development in urban and rural construction (Yang et al., 2024).

76 This study advances the understanding of the current status and driving factors of urban-rural PM
77 pollution improvement using interpretable machine learning methods. First, by integrating satellite
78 observation data, meteorological data, and geographic information, we use a multiple-output extreme
79 trees (MOET) model to capture the spatiotemporal distribution of PM (including PM₁₀ and PM_{2.5})
80 across China and assess the patterns of PM pollution improvement. We then use various machine learning
81 interpretability techniques, such as relative importance, tree interpreters, and SHAP values, to quantify
82 the contributions of anthropogenic emissions and meteorological changes to PM pollution improvement.
83 To investigate potential differences in the results between urban and rural areas, we use land use data to
84 distinguish urban from rural regions in eastern China. This study aims to address the following three
85 questions: (1) What are the spatio-temporal patterns of PM pollution improvement in urban and rural



86 areas of China? (2) What are the main driving factors behind the differences in PM pollution
87 improvement between urban and rural areas? (3) What are the specific contributions of each driving
88 factor to PM pollution improvement? Answering these questions is crucial for a comprehensive
89 understanding of the dynamics of urban and rural atmospheric particulate pollution control in China.

90 **2 Data and Methods**

91 **2.1 Satellite TOAR data and ground-based PM observations**

92 Previous studies have shown that satellite-observed top-of-atmosphere reflectance (TOAR) data
93 can be used to estimate near-surface air pollutants (Chen et al., 2024a; Yang et al., 2023; Song et al.,
94 2024). In particular, the TOAR data from the Himawari-8 satellite have demonstrated excellent
95 performance in pollutant estimation (Hu et al., 2022; Liu et al., 2019). The Advanced Himawari Imager
96 (AHI) on board the Himawari-8 satellite is an advanced passive observation instrument with 16
97 observation channels, providing a spatiotemporal resolution of up to 10 minutes and 0.5 km (Bessho et
98 al., 2016). Based on the sensitivity of the AHI sensor (Yoshida et al., 2018), three visible channels (0.46
99 μm , 0.51 μm , and 0.64 μm) and two near-infrared channels (0.86 μm and 2.3 μm) were used in this study.
100 TOAR data from the AHI imager were obtained from the Himawari Monitor P-Tree System data
101 download website of the Japan Meteorological Agency (<https://www.eorc.jaxa.jp/ptree/index.html>).

102 The ground-based PM data were provided by the China National Environmental Monitoring Center
103 (CEMC) (<http://www.cnemc.cn>) and were calibrated and quality controlled according to the Chinese
104 National Standard GB 3095-2012 (Ministry of Ecology and Environment of the People's Republic of
105 China, 2012). In this study, hourly mean PM₁₀ and PM_{2.5} data were collected from approximately 1,400
106 stations in eastern China (102-136°E, 16-56°N) for the period from 1 September 2015 to 31 August 2023.
107 Observations with PM_{2.5} concentrations above 600 $\mu\text{g}/\text{m}^3$ or PM₁₀ concentrations above 1,000 $\mu\text{g}/\text{m}^3$,
108 as well as those with concentrations below 1 $\mu\text{g}/\text{m}^3$, were excluded (Shi et al., 2024).

109 **2.2 Meteorological data and geographic information data**

110 Studies assessing the impact of meteorological factors on PM pollution have identified temperature,
111 humidity, and wind as the main variables influencing PM_{2.5} concentrations, with their effects
112 significantly outweighing those of other factors. Among these, temperature has the most significant and



stable influence (Chen et al., 2018b). In this study, meteorological data were obtained from the ERA-5 reanalysis dataset provided by the European Centre for Medium-Range Weather Forecasts (<https://cds.climate.copernicus.eu/cdsapp#!/dataset/>). The dataset includes boundary layer height (BLH), relative humidity (RH), surface pressure (SP), 2-metre air temperature (T2M), wind direction (WD), wind speed (WS), and net solar radiation at the surface (NSR), with spatial resolutions of $0.1^\circ \times 0.1^\circ$ or $0.25^\circ \times 0.25^\circ$ (Hersbach et al., 2020). Geographic information can also influence pollutant concentrations to some extent due to variations in meteorological conditions (Chen et al., 2018a; Chen et al., 2021). The geographic information data used in this study include elevation (HEIGHT), land cover type (LUCC), and population density (RK).

2.3 Data integration and development of the Multiple-Output Extreme Trees Model

The resolution of the meteorological and geographic information data was adjusted to $0.05^\circ \times 0.05^\circ$ using bilinear interpolation. All data were then matched with station data according to the $0.05^\circ \times 0.05^\circ$ grid of the Himawari-8 satellite. The specific matching method is described in detail in Chen et al. (2022c) and Song et al. (2022b).

The DOET model is developed on the basis of the Extreme Trees (ET) model (Geurts et al., 2006), which is capable of simultaneously handle multi-target variable output tasks. The ET model is similar to the Random Forest (RF) model, both of which consist of multiple decision trees. However, whereas the RF model randomly samples data with replacement, the ET model uses all available samples. After determining the samples and features, the ET model constructs decision trees based on optimal partition attributes. This process is repeated until a sufficient number of decision trees have been constructed to form the ET model. Finally, the average regression results of all decision trees in the ET are used as the final output. Several studies have confirmed that the ET model has excellent fitting performance (Qin et al., 2020; Zhang et al., 2022a; Chen et al., 2022a).

In this study, three model parameters were optimized: the number of trees (`n_estimators`), the maximum depth of the model (`max_depth`), and the minimum number of samples required to split a node (`min_samples_split`). After balancing the accuracy and efficiency of the model, these parameters were set to 70, 100, and 5, respectively. The model, which uses satellite observations, meteorological data, and geographical information to estimate near-surface PM concentrations, can be expressed as:



$$(PM_{10}, PM_{2.5})$$

$$= f(TOAR_{1,2,3,4,6}, BLH, RH, SP, T2M, WD, WS, Height, LUCC, RK, year, mon, doy, hour) \quad (1)$$

Here, f represents the DOET model, and $TOAR_{1,2,3,4,6}$ denotes the radiance values of the three visible channels (0.46 μm , 0.51 μm , and 0.64 μm) and the two near-infrared channels (0.86 μm and 2.3 μm). $BLH, RH, SP, T2M, WD$ and WS are meteorological variables, while $Height, LUCC$ and RK represent geographical information. The variables year, mon (month), doy (day of the year), and hour are temporal information reflecting the influence of anthropogenic emissions on PM pollution (Wei et al., 2020). Specifically, year and month (mon) are used to represent the interannual and intra-annual variations in anthropogenic emissions, respectively (Zhang et al., 2019a; Park et al., 2019). The estimation workflow is illustrated in Figure 1.

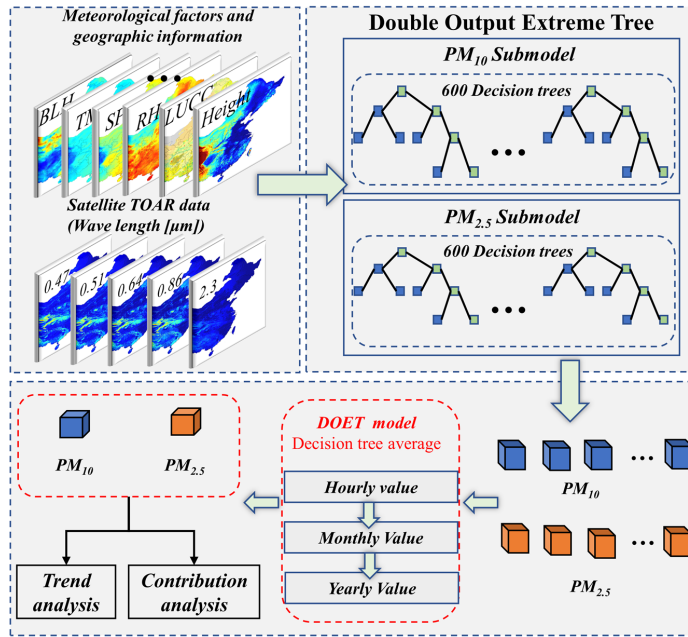


Figure 1. Workflow of PM data estimation and pollution driving factors assessment.

Model performance was evaluated using 10-fold cross-validation (Rodriguez et al., 2010), incorporating sample-based, space-based, and time-based validation methods (Wei et al., 2019). Evaluation metrics used included the coefficient of determination (R^2), root mean square error (RMSE), and mean absolute error (MAE) for both PM10 and PM2.5 (Chen et al., 2023).

$$R^2 = 1 - \frac{SS_{res}}{SS_{tot}} \quad (2)$$



$$MAE = \frac{1}{n} \sum_{i=1}^n |\hat{y}_i - y_i| \quad (3)$$

$$RMSE = \sqrt{\frac{1}{n} \sum_{i=1}^n (\hat{y}_i - y_i)^2} \quad (4)$$

2.4 Machine learning interpretability variables

To investigate the influence of potential driving factors on PM pollution improvement in eastern China, we employed relative importance (Berner et al., 2020), tree interpreter (Wang et al., 2022b), and SHAP values (Lundberg and Lee, 2017) to distinguish the contributions of meteorological changes and anthropogenic emissions to PM pollution improvement. Relative importance was assessed using the permutation importance value of the DOET model, defined as the average reduction in model accuracy when a single feature value is randomly shuffled (Yang et al., 2022).

The permutation importance of each variable was calculated using the “permutation_importance” library in Python. To reduce uncertainty, the training process was repeated 20 times for each grid point to obtain robust estimates of relative importance. The tree interpreter was applied using the ‘tree_interp_functions’ library in Python, which is designed for predictions based on decision tree ensemble models and facilitates the decomposition of each prediction into bias and feature contribution components. (<https://github.com/andosa/treeinterpreter/tree/master>).

SHAP values are based on Shapley value theory, which explains model predictions by calculating the relative contribution of each feature to the output (He et al., 2024). These values reflect not only the influence of features on individual samples but also indicate the positive and negative contributions of these influences. SHAP explanations can be applied to any machine learning model, including neural networks and ensemble models, and provide comprehensive and accurate interpretability results. Thus, the SHAP method provides superior explanations for both local and global model effects (Liu et al., 2023; Hou et al., 2022). In Python, “tree_SHAP” is specifically tailored for decision tree-based machine learning models, such as the Extreme Tree model, to provide greater accuracy and faster computation.

The interpretability variables described above were applied to the monthly averaged PM₁₀ and PM_{2.5} datasets generated by the DOET model.

2.5 Land cover type classification

Zhang et al. (2022b) proposed a method to differentiate urban and rural areas based on the gradient



185 of human land use pressure. In this study, the MCD12Q1 land cover map, with a spatial resolution of 500
186 meters was used. For grids measuring 5×5 km, urban and rural classifications were determined by the
187 coverage of specific land cover categories (e.g., urban land and cropland), which reflect the transition
188 from urban to rural areas and correspond to different levels of human activity. As shown in Table 1 and
189 Figure S1, urban areas in this study include both urban core areas and suburban regions, while rural areas
190 are categorized into six types: towns, high agricultural pressure areas, low agricultural pressure areas,
191 forests and grasslands.

192 **Table 1. Definitions of urban and rural land cover classes**

| Urban-Rural Land Cover Class | Definition |
|----------------------------------|---|
| Urban | 50%<Urban grid |
| Suburban | 25%<Urban grid<50% |
| Towns | 12.5%<Urban grid<25% |
| High Agricultural Pressure Areas | 50%<Cropland grid |
| Low Agricultural Pressure Areas | 12.5%< Cropland grid grid<50% |
| Forests | 50%<Forest grid |
| Grasslands | 50%<Grassland grid |
| Other | Remaining unclassified grids (e.g., desert or tundra) |

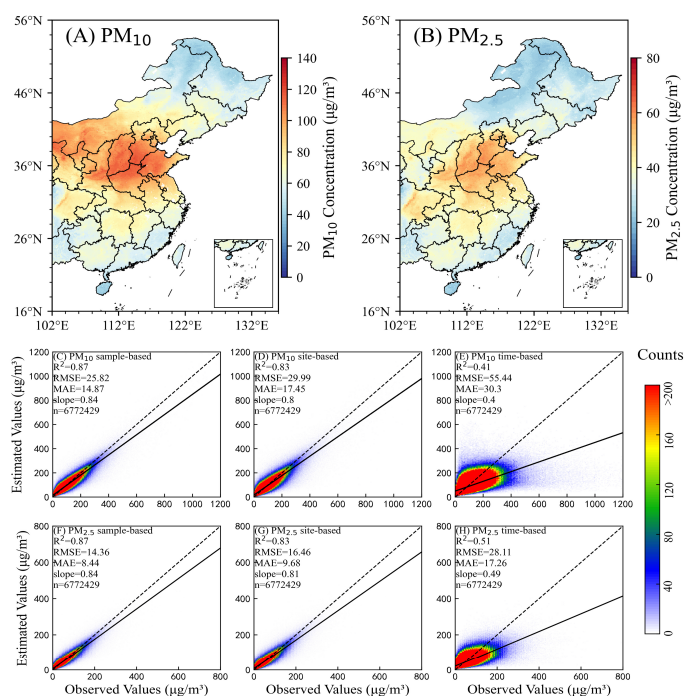
193 **3 Results**

194 **3.1 PM estimation model performance and PM distribution characteristics**

195 For the period from September 2015 to August 2023 in eastern China, a total of 6,772,429 samples
196 were matched. After parameter optimization and feature training, the optimal DOET model was derived,
197 and long-term time-series spatial distribution products for PM₁₀ and PM_{2.5} in eastern China were
198 generated. Figure 2 shows the results of 10-fold cross-validation based on sample, spatial and temporal
199 validations. Overall, the DOET model showed a high level of accuracy in the estimation of PM data. The
200 sample-based 10-fold cross-validation results (Figure 2C and 2F) yielded an R² of 0.87, with RMSE
201 (MAE) values of 25.82 (14.87) µg/m³ for PM₁₀ and 14.36 (8.44) µg/m³ for PM_{2.5}. The slope of the fitting
202 line between observed and estimated values was 0.84. The performance of the DOET model in this study
203 is comparable to that reported in other studies that estimated PM using Himawari-8 TOAR data (Wang
204 et al., 2021; Chen et al., 2024b; Yin et al., 2021).



205 The 10-fold cross-validation results based on spatial and temporal validation were slightly lower
206 than those based on samples (Figures 2D-E and 2G-H). Spatial validation assessed the performance of
207 the model in estimating PM concentrations in areas without monitoring stations, after training the model
208 with samples from areas with stations. Temporal validation involved training the model with samples
209 from specific years and testing it with data from years not used in training. For these two validation
210 methods, the R^2 values for PM_{10} were 0.83 and 0.41, with RMSE values of $29.99 \mu\text{g}/\text{m}^3$ and $55.44 \mu\text{g}/\text{m}^3$,
211 respectively. For $PM_{2.5}$, the R^2 values were 0.83 and 0.51, with RMSE values of $16.46 \mu\text{g}/\text{m}^3$ and $28.11 \mu\text{g}/\text{m}^3$,
212 respectively. The results of the sample-based, spatial, and temporal validation indicate that the
213 proposed DOET model exhibits robust stability.



214
215 **Figure 2. Spatial distribution of PM_{10} and $PM_{2.5}$ and cross validation results of the DOET model. The dashed**
216 **lines represent the 1:1 line, while the solid lines show the fitted line between observed and estimated values.**

217 By inputting TOAR, meteorological elements and geographical information into the optimally
218 parameterized DOET model, a pollutant estimation dataset for eastern China was generated for the period
219 September 2015 to August 2023. Due to the incomplete spatial coverage of TOAR data in different
220 months and hours (Song et al., 2024), the study first calculated monthly averages, which were then used
221 to derive annual averages. This step helps to minimize errors due to insufficient spatial coverage of the



222 samples (Ding et al., 2024). As shown in Figures 2A and 2B, the Beijing-Tianjin-Hebei region, the
223 Sichuan Basin, the Guanzhong region, and central China are hotspots for PM_{10} and $PM_{2.5}$ pollution (Wei
224 et al., 2021), with concentrations reaching up to $100 \mu\text{g}/\text{m}^3$ for PM_{10} and $60 \mu\text{g}/\text{m}^3$ for $PM_{2.5}$. In addition,
225 the Inner Mongolia region and northern Gansu, which are frequently affected by dust storms, are also
226 characterized by high PM_{10} concentrations (Li et al., 2012). Overall, the PM_{10} and $PM_{2.5}$
227 concentrations generated by the DOET model accurately reflect the spatial distribution characteristics of
228 PM in eastern China, and the estimation results are consistent with those of previous studies (Yang et al.,
229 2023; Chen et al., 2022b; Song et al., 2022a).

230 3.2 Urban-rural differences in PM pollution trends in recent years

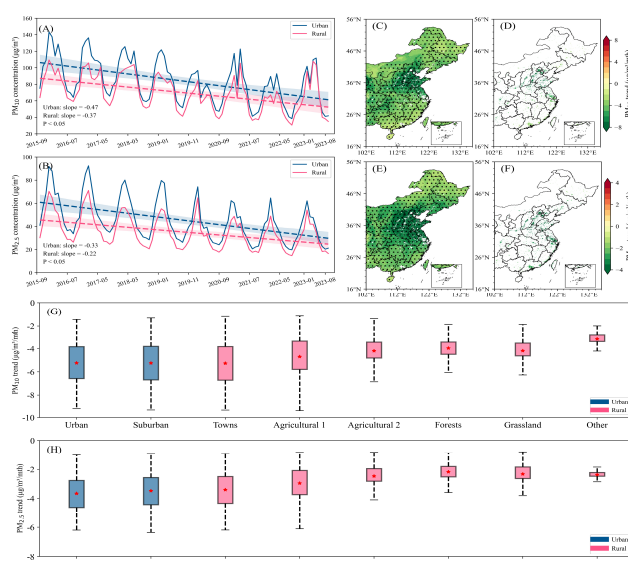
231 The spatial distribution characteristics of PM_{10} and $PM_{2.5}$ trends from 2015 to 2023 were analysed,
232 and the results (Figures 3C-F) show a remarkable improvement of PM pollution in eastern China, as
233 indicated by a significant decreasing trend in PM concentrations. The average decrease for PM_{10} was -
234 $4.1 \pm 1.1 \mu\text{g}/\text{m}^3/\text{month}$, while for $PM_{2.5}$, it was $-2.4 \pm 0.8 \mu\text{g}/\text{m}^3/\text{month}$. However, this widespread decrease
235 in PM concentrations showed considerable spatial heterogeneity between urban and rural areas. The
236 urban and rural decrease trends for PM_{10} were $-5.2 \pm 1.7 \mu\text{g}/\text{m}^3/\text{month}$ and $-4.1 \pm 1.1 \mu\text{g}/\text{m}^3/\text{month}$,
237 respectively, while for $PM_{2.5}$, they were $-3.6 \pm 1.1 \mu\text{g}/\text{m}^3/\text{month}$ and $-2.3 \pm 0.8 \mu\text{g}/\text{m}^3/\text{month}$, respectively.
238 This suggests that the decrease in PM concentrations in rural areas was close to the regional average in
239 eastern China, while the decrease in urban areas was more pronounced than the overall trend.

240 From a broader perspective of the changes in particulate matter concentrations in eastern China, the
241 urban decrease trends for PM_{10} and $PM_{2.5}$ were $-0.47 \mu\text{g}/\text{m}^3/\text{month}$ and $-0.33 \mu\text{g}/\text{m}^3/\text{month}$, respectively,
242 while the rural decrease trends were $-0.37 \mu\text{g}/\text{m}^3/\text{month}$ and $-0.22 \mu\text{g}/\text{m}^3/\text{month}$, respectively. These
243 results indicate that the reduction trend in rural areas was slower than in urban areas. By 2023, particulate
244 matter concentrations in urban areas had decreased from about $20 \mu\text{g}/\text{m}^3$ higher than in rural areas to
245 levels almost equal to those in rural areas.

246 Urban and rural areas, categorized by land cover type, comprised eight different categories. The
247 study assessed their respective roles in PM concentration reduction trends and found that all eight
248 categories showed declining PM trends. However, the regions with the highest PM reduction trends were
249 mainly four types: urban core areas, suburbs, towns and agricultural land 1 (high agricultural pressure).
250 In contrast, the reduction trends were less pronounced in agricultural land 2 (low agricultural pressure),



251 forests, grassland and other areas.



252
253 **Figure 3. Analysis of PM concentration trends in eastern China from September 2015 to August 2023. Panels**
254 **A, C, D, and G represent PM₁₀, while panels B, E, F, and H represent PM_{2.5}. In the legends of panels G-H,**
255 **blue indicates urban areas, and red indicates rural areas.**

256 The trends in PM₁₀ and PM_{2.5} concentrations were categorized into four levels based on percentiles:
257 slow decline (grid points with a decline trend below the 25th percentile), moderate decline (grid points
258 with a decline trend between the 25th and 75th percentiles), rapid decline (grid points with a decline
259 trend between the 75th and 95th percentiles), and sharp decline (grid points with a decline trend above
260 the 95th percentile). As shown in Figure 4, the regions with the most significant changes in urban and
261 rural PM trends are mainly concentrated in the Beijing-Tianjin-Hebei region, the Guanzhong region and
262 Central China.

263 In areas with slow and moderate declines, forests and grasslands accounted for the highest
264 proportions, ranging from 20.5% to 31.5% and 27.7% to 36.5%, respectively, followed by the first and
265 second types of agricultural land, which accounted for about 20%. In regions with rapid decline, the first
266 type of agricultural land had the highest proportion, ranging from 30 to 40%. Urban core, suburban and
267 rural areas had higher proportions in the fast decline regions, accounting for 6.7%, 7.0% and 8.8% of the
268 PM₁₀ decline trends and 9.5%, 7.5% and 8.8% of the PM_{2.5} decline trends respectively. In particular,
269 the first type of agricultural land had the largest share in the strong decrease regions.

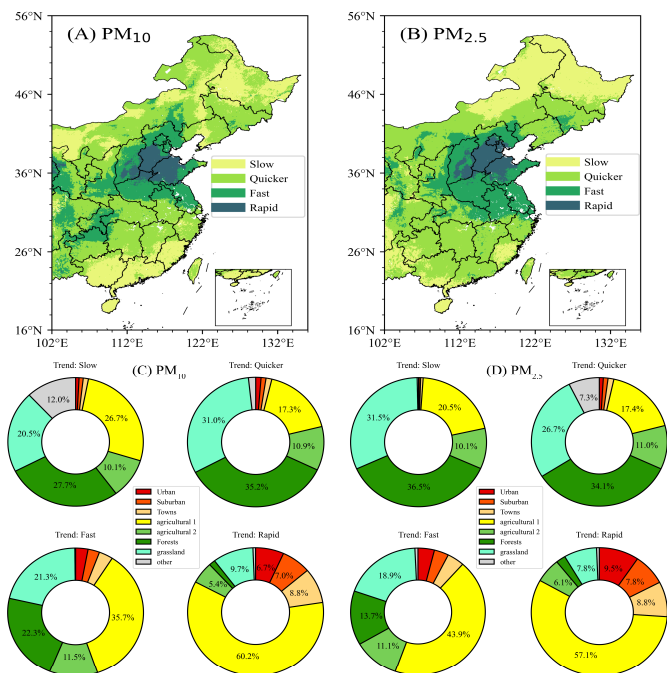


Figure 4. Spatial distribution of particulate matter trend percentiles and pie charts. The individual color scales in the figure represent different areas.

3.3 Assessing potential driving factors for PM pollution improvement and quantifying their contributions

A DOET model based on monthly PM data was developed to identify the key drivers of urban and rural greening changes in China. Monthly mean PM_{10} and $PM_{2.5}$ concentrations were correlated with meteorological factors and two temporal variables (year and month) representing the effects of meteorological changes and anthropogenic influences, respectively (see Methods for details). The model was cross-validated using a random training set (70%) and a validation set (30%). As shown in Figure S2, the DOET model explains more than 60% of the PM_{10} trends and 80% of the $PM_{2.5}$ trends in eastern China.

The relative importance of each variable in the DOET model was determined using the permutation_importance library. Inter-annual variability, intra-annual variability, air pressure and temperature were identified as significant contributors to the improvement of urban and rural PM pollution in eastern China (relative importance > 10%). Among them, interannual variability was the most influential factor for PM_{10} ($28.3 \pm 12\%$), followed by temperature ($21.1 \pm 15\%$) (Figure 5A). In



contrast, for $PM_{2.5}$, interannual variability ranked second ($32 \pm 13.2\%$), while temperature had a stronger effect ($>40\%$) (Figure 5B). The spatial distribution of the relative importance of the four main contributing factors, shown in Figures 5C-R, indicates that regions with high relative importance values overlapped with PM pollution hotspots. Furthermore, as shown in Figure S3, the driving factors for urban and rural PM pollution improvement differed significantly between land cover types.

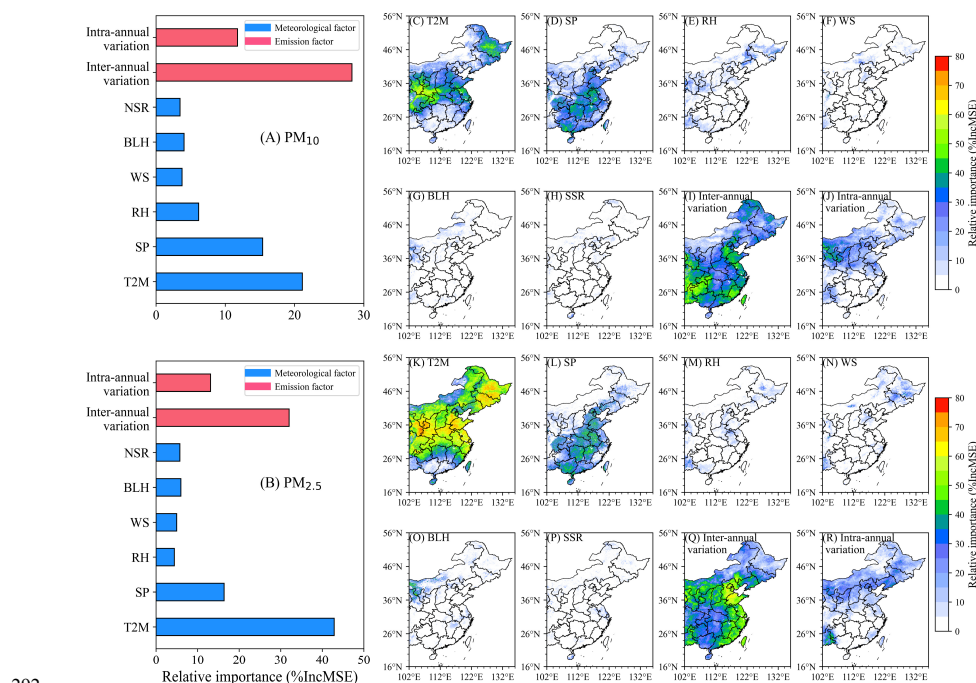


Figure 5. Spatial distribution of the relative influence of each variable on PM pollution. In panels (A-B), the red variables are related to emissions and the blue variables are related to meteorology.

The relative contributions of each variable in the DOET model to the PM concentration values were obtained using the permutation_importance library. The results showed that the improvement in urban and rural PM pollution was primarily driven by interannual variation (Figure 5), followed by temperature, which is consistent with the relative importance results in Figure 5. Figures S4-S5 illustrate how variations in the values of the driving factors influence their relative contributions to PM concentrations. In particular, PM concentrations showed a clear inverse relationship with temperature and interannual variations, especially for $PM_{2.5}$. Relative humidity also showed clear differences in its contribution to PM_{10} and $PM_{2.5}$: lower relative humidity was associated with higher PM_{10} concentrations, whereas higher $PM_{2.5}$ concentrations were associated with higher relative humidity. The scatter plots illustrating the



relationships between other variables and their relative contributions to PM are shown in Figures S4-S5.

Figure 6 shows the relative contributions of each variable, with the spatial distribution patterns of interannual variations being particularly noteworthy. For PM₁₀, regions such as Guanzhong, North China, and Inner Mongolia were more susceptible to the influence of interannual variations. We hypothesize that the improvement in PM₁₀ pollution be due not only be attributed to anthropogenic emission reductions but also to sandstorm events in recent years, which are important sources of PM₁₀ (Wang et al., 2024c). However, the explanatory power of the model for PM₁₀ trends in these areas remains relatively low, suggesting the need for further investigation into the specific causes. For PM_{2.5}, the impact of interannual variability was observed mainly in the Guanzhong region, North China, and the Sichuan Basin, all of which are key areas for pollution control (Wang et al., 2022a; Yu et al., 2022). Contrary to the relative importance results, the dominant factor driving the improvement in urban and rural PM pollution was the influence of interannual variability (Figure S6), with other variables showing varying effects across different land cover types.

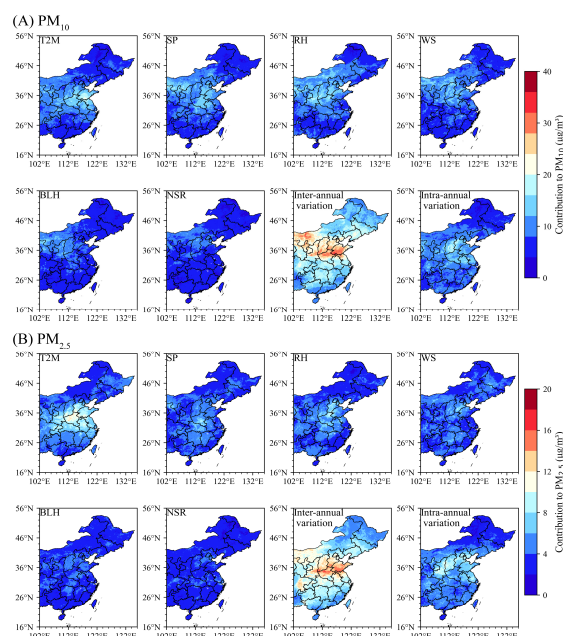
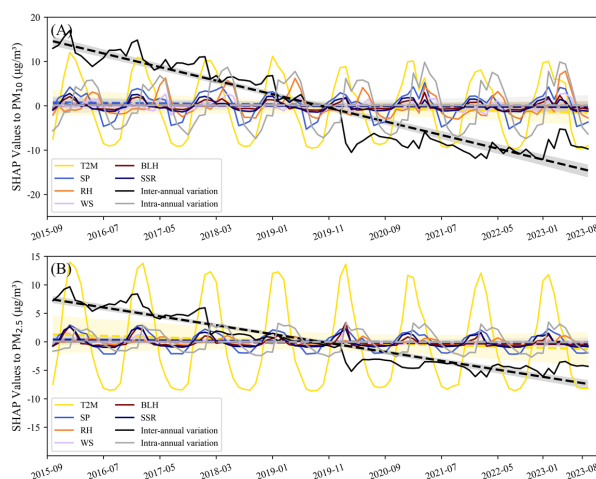


Figure 6. The spatial distribution of the relative contributions of each variable to PM pollution

Finally, the “tree_SHAP” tool was used to decompose the SHAP values of each variable in the DOET model. By analyzing the positive and negative changes in the SHAP values, the influence of each variable on the PM pollution improvement - whether positive or negative - was quantified, thus



322 complementing the assessment of driving factor contributions (Li et al., 2024a). As shown in Figure 7,
323 the SHAP values show a strong negative correlation between PM concentrations and the contribution of
324 interannual variability in eastern China. In particular, during the transition from 2019 to 2020, the
325 contribution of interannual variations to PM concentrations shifted critically from positive to negative.
326 Interestingly, despite the high relative importance and contribution of some variables, their SHAP values
327 showed periodic fluctuations, alternating between positive and negative, such as for temperature (with a
328 negative contribution in summer and a positive one in winter). This suggests that meteorological factors
329 influence PM concentrations in a periodic manner, while the only factor that consistently contributes to
330 the improvement of PM pollution is the interannual variation driven by anthropogenic influences.



331
332 **Figure 7. The SHAP values of each variable for PM. The solid line represents the SHAP values, and the dashed**
333 **line indicates their trend of change.**

334 3.5 Trends in the contribution of driving factors to PM pollution improvement

335 To further investigate the influence of potential driving factors on PM concentrations, we conducted
336 a detailed analysis of the trends in the contributions of each variable was performed. As shown in Figures
337 S7-S10, the monthly trends in the relative contributions and SHAP values of each variable were examined,
338 categorized into significant changes ($p < 0.05$) and non-significant changes ($p > 0.05$). For the relative
339 contributions (including PM_{10} and $PM_{2.5}$), with the exception of interannual variations, all other variables
340 showed a decreasing trend, although some regions showed an increasing trend. However, the contribution
341 of interannual variability showed a significant decrease, indicating a reduced capacity of anthropogenic



emissions to trigger PM pollution events. This phenomenon is more pronounced for the trends in SHAP values. In particular, only the contribution of interannual variations showed a significant decreasing trend, while the other variables showed non-significant decreasing trends, mainly due to the periodic variations in their contributions, as shown in Figure 7. This shows that the impact of a variable on PM pollution cannot only be assessed on the basis of its relative contribution, but its positive or negative influence on the improvement of PM pollution must also be considered.

Given the significant decrease in the contribution of interannual variation, we further compared its trends across different land cover types in urban and rural areas, as this variable plays the most important role in PM pollution improvement. As shown in Figure 8 (A-B), the trends in relative contributions for both PM_{10} and $PM_{2.5}$ did not differ significantly between the eight land cover types, although urban areas showed the highest rate of decrease. However, the trends in SHAP values shown in Figures 8 (C-D) revealed that the reduction in the contribution of interannual variation was most pronounced in urban core areas, suburban areas, and towns. In contrast, the decrease in interannual contributions was more pronounced in agricultural areas than in urban areas, while other rural areas showed a weaker influence of interannual variations on PM pollution improvement. These results suggest that the improvement in PM pollution in urban areas is more closely related to anthropogenic influences, whereas this relationship is less pronounced in rural areas.

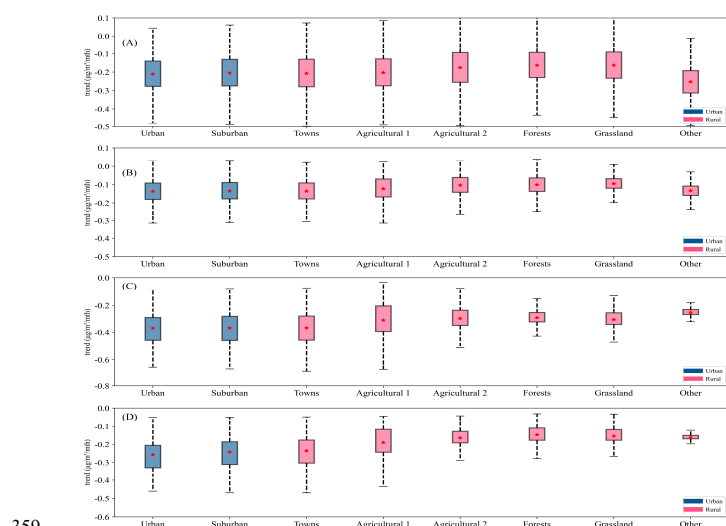


Figure 8. Trends in the relative contribution (A-B) and SHAP values (C-D) of interannual variability of different land cover types. A and C represent the case for PM_{10} , while B and D represent the case for $PM_{2.5}$. In the legend, blue represents urban areas, and red represents rural areas.



363 4 Discussion and conclusion

364 Due to the predominant distribution of environmental quality monitoring stations in urban areas
365 (Park et al., 2020), discussions on air pollution patterns between urban and rural regions have been
366 limited (Hammer et al., 2020). In this study, we used a regression-based machine learning DOET
367 algorithm to integrate station-observed PM concentrations, satellite-observed TOAR, meteorological
368 factors, and geographic information data. This approach enabled us to generate long-term, high spatio-
369 temporal resolution datasets of near-surface PM₁₀ and PM_{2.5}, with a spatial resolution of 5 km, an hourly
370 temporal resolution, and coverage across the entire eastern China region. Using the generated PM data
371 in conjunction with a constructed urban-rural land type framework, we successfully captured the broad
372 trends and patterns of PM₁₀ and PM_{2.5} concentration changes from urban and suburban areas to different
373 types of rural regions.

374 Based on the estimated dataset and interpretable parameters, the study identified significant large-
375 scale improvements in PM pollution in eastern China from 2015 to 2023, indicating notable
376 achievements from the implementation of clean air measures. The study noted that the second phase of
377 the clean air action plan, implemented from 2018 to 2020, also produced positive results, following the
378 success of the first phase from 2013 to 2017 (Geng et al., 2024). Our results show that under the urban-
379 rural framework, PM reductions are generally higher in urban areas than in rural areas. However, the
380 highly polluted agricultural areas in rural regions also showed significant improvements in PM pollution.
381 In fact, during air pollution prevention and control efforts, China's main emission reduction measures
382 focused on coal consumption and energy-intensive industries such as steel and cement, and these
383 measures were often effective in urban areas (Yun et al., 2020; Huang et al., 2014b; Wang et al., 2013).
384 This does not mean that rural areas have been neglected, as evidenced by reductions in biomass burning
385 (Shen et al., 2019). The finding that interannual variability is the main driver of PM pollution
386 improvement is consistent with these facts. It is worth noting that the rate of PM concentration decline
387 is faster in urban areas than in rural areas, bringing the concentration levels of the two areas closer
388 together. Given the more pronounced decrease in the contribution of inter-annual variations in urban
389 areas, future efforts to prevent and control air pollution should maintain the current intensity or balance
390 investments between urban and rural areas.

391 Our results indicate that meteorological factors with distinct seasonal variations, such as



392 temperature, boundary layer height, and relative humidity, have a cyclical influence on PM pollution.
393 For example, summer weather conditions, such as abundant precipitation, high relative humidity and
394 abundant water vapour favour PM dispersion, while winter weather conditions are less conducive to
395 pollutant dispersion and spring is often characterised by frequent dust events. Therefore, due to their
396 periodic positive and negative contributions and variability, meteorological conditions do not provide
397 stable improvements in PM pollution. Moreover, the contribution of meteorological conditions to PM
398 concentrations does not show a significant trend. Thus, given the high contribution of inter-annual
399 variability to the improvement of PM pollution, the impact of meteorological conditions on the inter-
400 annual variability of PM pollution in China should not be overemphasised.

401 Although this study evaluated the patterns of PM pollution improvement and its driving factors in
402 urban and rural areas of eastern China, the contribution of interannual variations driven by anthropogenic
403 influences was represented by a time variable in our analysis. In the future, key factors driving changes
404 in air pollutants, such as energy management, urban traffic management, agricultural nitrogen deposition
405 effects and biomass burning, need to be further incorporated into the attribution analysis to distinguish
406 and quantify the contributions of different anthropogenic emission reduction measures to PM pollution
407 improvement. Given the different drivers of PM pollution improvement in urban and rural areas, it is
408 essential to implement tailored strategies in both regions to achieve more effective and comprehensive
409 air pollution prevention and control measures in the future.

410 **Data availability**

411 The hourly ground station observations of near-surface PM_{10} and $PM_{2.5}$ concentrations are obtained from
412 the China National Environmental Monitoring Center (CNEMC), which can be accessed on its official
413 website (<http://www.cnemc.cn/en/>). Himawari-8 TOAR data provided by the Japan Meteorological
414 Agency, download from: <http://www.eorc.jaxa.jp/ptree/index.html>. Meteorological variables were
415 derived from the reanalysis data set provided by the European Centre for Medium-Range Weather
416 Forecasts (ECMWF) (<https://cds.climate.copernicus.eu/cdsapp#!/search?type=dataset>). MODIS Land
417 use/cover change (LUCC) product can be downloaded from
418 <https://doi.org/10.5067/MODIS/MCD12C1.061>. The 2015 UN-adjusted population density data (RK)
419 can be downloaded from <https://doi.org/10.7927/H4PN93PB>. SRTM-3 elevation data jointly measured



420 by NASA and the U.S. Department of Defense's National Imagery and Mapping Agency (NIMA)
421 (HEIGHT) can be downloaded from <https://doi.org/10.5067/MEaSURES/SRTM/SRTMGL3.003>.

422 **Code availability**

423 The codes are available from the corresponding author upon request.

424 **Acknowledgements**

425 We would like to express our gratitude to the China National Environmental Monitoring Center,
426 Japan Meteorological Agency, European Centre for Medium-Range Weather Forecasts, and NASA
427 for their datasets.

428 **Financial support**

429 The work was supported by the Noncommunicable Chronic Diseases-National Science and Technology
430 Major Project (Grant number 2024ZD0531600), the National Natural Science Foundation of China
431 (Grant number 42427803), the Gansu Provincial Science and Technology Plan (Grant number
432 25RCKA024), and the Fundamental Research Funds for the Central Universities (Grant number lzujbky-
433 2023-ey10).

434 **Author contributions**

435 Z.S.: Software, Methodology, Data curation, Writing-Original draft preparation, Formal Analysis,
436 Visualization. B.C.: Conceptualization, Methodology, Writing-Reviewing and Editing, Resources.

437 **Competing interests**

438 The authors declare that they have no conflict of interest.

439 **References**

440 An, Z., Huang, R.-J., Zhang, R., Tie, X., Li, G., Cao, J., Zhou, W., Shi, Z., Han, Y., Gu, Z., and Ji, Y.:
441 Severe haze in northern China: A synergy of anthropogenic emissions and atmospheric processes,
442 Proceedings of the National Academy of Sciences, 116, 8657-8666,
443 <https://doi.org/10.1073/pnas.1900125116>, 2019.
444 Apte, J. S., Marshall, J. D., Cohen, A. J., and Brauer, M.: Addressing Global Mortality from Ambient



- PM2.5, *Environmental Science & Technology*, 49, 8057-8066, <https://doi.org/10.1021/acs.est.5b01236>, 2015.
- Berner, L. T., Massey, R., Jantz, P., Forbes, B. C., Macias-Fauria, M., Myers-Smith, I., Kumpula, T., Gauthier, G., Andreu-Hayles, L., Gaglioti, B. V., Burns, P., Zetterberg, P., D'Arrigo, R., and Goetz, S. J.: Summer warming explains widespread but not uniform greening in the Arctic tundra biome, *Nature Communications*, 11, 4621, <https://doi.org/10.1038/s41467-020-18479-5>, 2020.
- Bessho, K., Date, K., Hayashi, M., Ikeda, A., Imai, T., Inoue, H., Kumagai, Y., Miyakawa, T., Murata, H., Ohno, T., Okuyama, A., Oyama, R., Sasaki, Y., Shimazu, Y., Shimoji, K., Sumida, Y., Suzuki, M., Taniguchi, H., Tsuchiyama, H., Uesawa, D., Yokota, H., and Yoshida, R.: An Introduction to Himawari-8/9—Japan's New-Generation Geostationary Meteorological Satellites, *Journal of the Meteorological Society of Japan. Ser. II*, 94, 151-183, <https://doi.org/10.2151/jmsj.2016-009>, 2016.
- Brauer, M., Freedman, G., Frostad, J., van Donkelaar, A., Martin, R. V., Dentener, F., Dingenen, R. v., Estep, K., Amini, H., Apte, J. S., Balakrishnan, K., Barregard, L., Broday, D., Feigin, V., Ghosh, S., Hopke, P. K., Knibbs, L. D., Kokubo, Y., Liu, Y., Ma, S., Morawska, L., Sangrador, J. L. T., Shaddick, G., Anderson, H. R., Vos, T., Forouzanfar, M. H., Burnett, R. T., and Cohen, A.: Ambient Air Pollution Exposure Estimation for the Global Burden of Disease 2013, *Environmental Science & Technology*, 50, 79-88, <https://doi.org/10.1021/acs.est.5b03709>, 2016.
- Burnett, R., Chen, H., Szyszkowicz, M., Fann, N., Hubbell, B., Pope, C. A., Apte, J. S., Brauer, M., Cohen, A., Weichenhal, S., Coggins, J., Di, Q., Brunekreef, B., Frostad, J., Lim, S. S., Kan, H., Walker, K. D., Thurston, G. D., Hayes, R. B., Lim, C. C., Turner, M. C., Jerrett, M., Krewski, D., Gapstur, S. M., Diver, W. R., Ostro, B., Goldberg, D., Crouse, D. L., Martin, R. V., Peters, P., Pinault, L., Tjepkema, M., van Donkelaar, A., Villeneuve, P. J., Miller, A. B., Yin, P., Zhou, M., Wang, L., Janssen, N. A. H., Marra, M., Atkinson, R. W., Tsang, H., Quoc Thach, T., Cannon, J. B., Allen, R. T., Hart, J. E., Laden, F., Cesaroni, G., Forastiere, F., Weinmayr, G., Jaensch, A., Nagel, G., Concin, H., and Spadaro, J. V.: Global estimates of mortality associated with long-term exposure to outdoor fine particulate matter, *Proceedings of the National Academy of Sciences*, 115, 9592-9597, <https://doi.org/10.1073/pnas.1803222115>, 2018.
- Burnett Richard, T., Pope, C. A., Ezzati, M., Olives, C., Lim Stephen, S., Mehta, S., Shin Hwashin, H., Singh, G., Hubbell, B., Brauer, M., Anderson, H. R., Smith Kirk, R., Balmes John, R., Bruce Nigel, G., Kan, H., Laden, F., Prüss-Ustün, A., Turner Michelle, C., Gapstur Susan, M., Diver, W. R., and Cohen, A.: An Integrated Risk Function for Estimating the Global Burden of Disease Attributable to Ambient Fine Particulate Matter Exposure, *Environmental Health Perspectives*, 122, 397-403, <https://doi.org/10.1289/ehp.1307049>, 2014.
- Cao, B. and Yin, Z.: Future atmospheric circulations benefit ozone pollution control in Beijing-Tianjin-Hebei with global warming, *Science of The Total Environment*, 743, 140645, <https://doi.org/10.1016/j.scitotenv.2020.140645>, 2020.
- Chen, B., Hu, J., and Wang, Y.: Synergistic observation of FY-4A&4B to estimate CO concentration in China: combining interpretable machine learning to reveal the influencing mechanisms of CO variations, *npj Climate and Atmospheric Science*, 7, 9, <https://doi.org/10.1038/s41612-023-00559-0>, 2024a.
- Chen, B., Song, Z., Pan, F., and Huang, Y.: Obtaining vertical distribution of PM2.5 from CALIOP data and machine learning algorithms, *Science of The Total Environment*, 805, 150338, <https://doi.org/10.1016/j.scitotenv.2021.150338>, 2022a.
- Chen, B., Song, Z., Shi, B., and Li, M.: An interpretable deep forest model for estimating hourly PM10 concentration in China using Himawari-8 data, *Atmospheric Environment*, 268, 118827, <https://doi.org/10.1016/j.atmosenv.2021.118827>, 2022b.



- 489 Chen, B., Wang, Y., Huang, J., Zhao, L., Chen, R., Song, Z., and Hu, J.: Estimation of near-surface ozone
490 concentration and analysis of main weather situation in China based on machine learning model and
491 Himawari-8 TOAR data, *Science of The Total Environment*, 864, 160928,
492 <https://doi.org/10.1016/j.scitotenv.2022.160928>, 2023.
- 493 Chen, B., Song, Z., Huang, J., Zhang, P., Hu, X., Zhang, X., Guan, X., Ge, J., and Zhou, X.: Estimation
494 of Atmospheric PM10 Concentration in China Using an Interpretable Deep Learning Model and Top-of-
495 the-Atmosphere Reflectance Data From China's New Generation Geostationary Meteorological Satellite,
496 FY-4A, *Journal of Geophysical Research: Atmospheres*, 127, e2021JD036393,
497 <https://doi.org/10.1029/2021JD036393>, 2022c.
- 498 Chen, C.-C., Wang, Y.-R., Yeh, H.-Y., Lin, T.-H., Huang, C.-S., and Wu, C.-F.: Estimating monthly PM2.5
499 concentrations from satellite remote sensing data, meteorological variables, and land use data using
500 ensemble statistical modeling and a random forest approach, *Environmental Pollution*, 291, 118159,
501 <https://doi.org/10.1016/j.envpol.2021.118159>, 2021.
- 502 Chen, G., Li, S., Knibbs, L. D., Hamm, N. A. S., Cao, W., Li, T., Guo, J., Ren, H., Abramson, M. J., and
503 Guo, Y.: A machine learning method to estimate PM2.5 concentrations across China with remote sensing,
504 meteorological and land use information, *Science of The Total Environment*, 636, 52-60,
505 <https://doi.org/10.1016/j.scitotenv.2018.04.251>, 2018a.
- 506 Chen, J., Li, Z., Lv, M., Wang, Y., Wang, W., Zhang, Y., Wang, H., Yan, X., Sun, Y., and Cribb, M.:
507 Aerosol hygroscopic growth, contributing factors, and impact on haze events in a severely polluted
508 region in northern China, *Atmos. Chem. Phys.*, 19, 1327-1342, [https://doi.org/10.5194/acp-19-1327-](https://doi.org/10.5194/acp-19-1327-2019)
509 [2019](https://doi.org/10.5194/acp-19-1327-2019), 2019a.
- 510 Chen, L., Zhu, J., Liao, H., Yang, Y., and Yue, X.: Meteorological influences on PM2.5 and O3 trends
511 and associated health burden since China's clean air actions, *Science of The Total Environment*, 744,
512 140837, <https://doi.org/10.1016/j.scitotenv.2020.140837>, 2020a.
- 513 Chen, S., Guo, J., Song, L., Li, J., Liu, L., and Cohen, J. B.: Inter-annual variation of the spring haze
514 pollution over the North China Plain: Roles of atmospheric circulation and sea surface temperature,
515 *International Journal of Climatology*, 39, 783-798, <https://doi.org/10.1002/joc.5842>, 2019b.
- 516 Chen, X., Zhang, W., He, J., Zhang, L., Guo, H., Li, J., and Gu, X.: Mapping PM2.5 concentration from
517 the top-of-atmosphere reflectance of Himawari-8 via an ensemble stacking model, *Atmospheric*
518 *Environment*, 330, 120560, <https://doi.org/10.1016/j.atmosenv.2024.120560>, 2024b.
- 519 Chen, Z., Xie, X., Cai, J., Chen, D., Gao, B., He, B., Cheng, N., and Xu, B.: Understanding
520 meteorological influences on PM2.5 concentrations across China: a temporal and spatial perspective,
521 *Atmos. Chem. Phys.*, 18, 5343-5358, <https://doi.org/10.5194/acp-18-5343-2018>, 2018b.
- 522 Chen, Z., Chen, D., Zhao, C., Kwan, M.-p., Cai, J., Zhuang, Y., Zhao, B., Wang, X., Chen, B., Yang, J.,
523 Li, R., He, B., Gao, B., Wang, K., and Xu, B.: Influence of meteorological conditions on PM2.5
524 concentrations across China: A review of methodology and mechanism, *Environment International*, 139,
525 105558, <https://doi.org/10.1016/j.envint.2020.105558>, 2020b.
- 526 Cheng, J., Tong, D., Zhang, Q., Liu, Y., Lei, Y., Yan, G., Yan, L., Yu, S., Cui, R. Y., Clarke, L., Geng, G.,
527 Zheng, B., Zhang, X., Davis, S. J., and He, K.: Pathways of China's PM2.5 air quality 2015–2060 in the
528 context of carbon neutrality, *National Science Review*, 8, nwab078, <https://doi.org/10.1093/nsr/nwab078>,
529 2021.
- 530 Cohen, A. J., Brauer, M., Burnett, R., Anderson, H. R., Frostad, J., Estep, K., Balakrishnan, K.,
531 Brunekreef, B., Dandona, L., Dandona, R., Feigin, V., Freedman, G., Hubbell, B., Jobling, A., Kan, H.,
532 Knibbs, L., Liu, Y., Martin, R., Morawska, L., Pope, C. A., Shin, H., Straif, K., Shaddick, G., Thomas,



- 533 M., van Dingenen, R., van Donkelaar, A., Vos, T., Murray, C. J. L., and Forouzanfar, M. H.: Estimates
534 and 25-year trends of the global burden of disease attributable to ambient air pollution: an analysis of
535 data from the Global Burden of Diseases Study 2015, *The Lancet*, 389, 1907-1918,
536 [https://doi.org/10.1016/S0140-6736\(17\)30505-6](https://doi.org/10.1016/S0140-6736(17)30505-6), 2017.
- 537 Ding, Y., Li, S., Xing, J., Li, X., Ma, X., Song, G., Teng, M., Yang, J., Dong, J., and Meng, S.: Retrieving
538 hourly seamless PM_{2.5} concentration across China with physically informed spatiotemporal connection,
539 *Remote Sensing of Environment*, 301, 113901, <https://doi.org/10.1016/j.rse.2023.113901>, 2024.
- 540 Geng, G., Xiao, Q., Zheng, Y., Tong, D., Zhang, Y., Zhang, X., Zhang, Q., He, K., and Liu, Y.: Impact of
541 China's Air Pollution Prevention and Control Action Plan on PM_{2.5} chemical composition over eastern
542 China, *Science China Earth Sciences*, 62, 1872-1884, <https://doi.org/10.1007/s11430-018-9353-x>, 2019.
- 543 Geng, G., Liu, Y., Liu, Y., Liu, S., Cheng, J., Yan, L., Wu, N., Hu, H., Tong, D., Zheng, B., Yin, Z., He,
544 K., and Zhang, Q.: Efficacy of China's clean air actions to tackle PM_{2.5} pollution between 2013 and
545 2020, *Nature Geoscience*, 17, 987-994, 10.1038/s41561-024-01540-z, 2024.
- 546 Geurts, P., Ernst, D., and Wehenkel, L.: Extremely randomized trees, *Machine Learning*, 63, 3-42,
547 <https://doi.org/10.1007/s10994-006-6226-1>, 2006.
- 548 Gui, K., Che, H., Wang, Y., Wang, H., Zhang, L., Zhao, H., Zheng, Y., Sun, T., and Zhang, X.: Satellite-
549 derived PM_{2.5} concentration trends over Eastern China from 1998 to 2016: Relationships to emissions
550 and meteorological parameters, *Environmental Pollution*, 247, 1125-1133,
551 <https://doi.org/10.1016/j.envpol.2019.01.056>, 2019.
- 552 Hammer, M. S., van Donkelaar, A., Li, C., Lyapustin, A., Sayer, A. M., Hsu, N. C., Levy, R. C., Garay,
553 M. J., Kalashnikova, O. V., Kahn, R. A., Brauer, M., Apte, J. S., Henze, D. K., Zhang, L., Zhang, Q.,
554 Ford, B., Pierce, J. R., and Martin, R. V.: Global Estimates and Long-Term Trends of Fine Particulate
555 Matter Concentrations (1998–2018), *Environmental Science & Technology*, 54, 7879-7890,
556 10.1021/acs.est.0c01764, 2020.
- 557 He, J., Gong, S., Yu, Y., Yu, L., Wu, L., Mao, H., Song, C., Zhao, S., Liu, H., Li, X., and Li, R.: Air
558 pollution characteristics and their relation to meteorological conditions during 2014–2015 in major
559 Chinese cities, *Environmental Pollution*, 223, 484-496, <https://doi.org/10.1016/j.envpol.2017.01.050>,
560 2017.
- 561 He, Q., Cao, J., Saide, P. E., Ye, T., and Wang, W.: Unraveling the Influence of Satellite-Observed Land
562 Surface Temperature on High-Resolution Mapping of Ground-Level Ozone Using Interpretable Machine
563 Learning, *Environmental Science & Technology*, 58, 15938-15948,
564 <https://doi.org/10.1021/acs.est.4c02926>, 2024.
- 565 Hersbach, H., Bell, B., Berrisford, P., Hirahara, S., Horányi, A., Muñoz-Sabater, J., Nicolas, J., Peubey,
566 C., Radu, R., Schepers, D., Simmons, A., Soci, C., Abdalla, S., Abellan, X., Balsamo, G., Bechtold, P.,
567 Biavati, G., Bidlot, J., Bonavita, M., De Chiara, G., Dahlgren, P., Dee, D., Diamantakis, M., Dragani, R.,
568 Flemming, J., Forbes, R., Fuentes, M., Geer, A., Haimberger, L., Healy, S., Hogan, R. J., Hólm, E.,
569 Janisková, M., Keeley, S., Laloyaux, P., Lopez, P., Lupu, C., Radnoti, G., de Rosnay, P., Rozum, I.,
570 Vamborg, F., Villaume, S., and Thépaut, J.-N.: The ERA5 global reanalysis, *Quarterly Journal of the*
571 *Royal Meteorological Society*, 146, 1999-2049, <https://doi.org/10.1002/qj.3803>, 2020.
- 572 Hou, L., Dai, Q., Song, C., Liu, B., Guo, F., Dai, T., Li, L., Liu, B., Bi, X., Zhang, Y., and Feng, Y.:
573 Revealing Drivers of Haze Pollution by Explainable Machine Learning, *Environmental Science &*
574 *Technology Letters*, 9, 112-119, <https://doi.org/10.1021/acs.estlett.1c00865>, 2022.
- 575 Hu, Y., Zeng, C., Li, T., and Shen, H.: Performance comparison of Fengyun-4A and Himawari-8 in PM_{2.5}
576 estimation in China, *Atmospheric Environment*, 271, 118898,



- 577 <https://doi.org/10.1016/j.atmosenv.2021.118898>, 2022.
- 578 Huang, R.-J., Zhang, Y., Bozzetti, C., Ho, K.-F., Cao, J.-J., Han, Y., Daellenbach, K. R., Slowik, J. G.,
579 Platt, S. M., Canonaco, F., Zotter, P., Wolf, R., Pieber, S. M., Bruns, E. A., Crippa, M., Ciarelli, G.,
580 Piazzalunga, A., Schwikowski, M., Abbaszade, G., Schnelle-Kreis, J., Zimmermann, R., An, Z., Szidat,
581 S., Baltensperger, U., Haddad, I. E., and Prévôt, A. S. H.: High secondary aerosol contribution to
582 particulate pollution during haze events in China, *Nature*, 514, 218-222,
583 <https://doi.org/10.1038/nature13774>, 2014a.
- 584 Huang, Y., Shen, H., Chen, H., Wang, R., Zhang, Y., Su, S., Chen, Y., Lin, N., Zhuo, S., Zhong, Q., Wang,
585 X., Liu, J., Li, B., Liu, W., and Tao, S.: Quantification of Global Primary Emissions of PM_{2.5}, PM₁₀,
586 and TSP from Combustion and Industrial Process Sources, *Environmental Science & Technology*, 48,
587 13834-13843, 10.1021/es503696k, 2014b.
- 588 Li, J., Wang, Z., Zhuang, G., Luo, G., Sun, Y., and Wang, Q.: Mixing of Asian mineral dust with
589 anthropogenic pollutants over East Asia: a model case study of a super-duststorm in March 2010, *Atmos.*
590 *Chem. Phys.*, 12, 7591-7607, <https://doi.org/10.5194/acp-12-7591-2012>, 2012.
- 591 Li, W., Wang, C., Wang, H., Chen, J., Yuan, C., Li, T., Wang, W., Shen, H., Huang, Y., Wang, R., Wang,
592 B., Zhang, Y., Chen, H., Chen, Y., Tang, J., Wang, X., Liu, J., Coveney, R. M., and Tao, S.: Distribution
593 of atmospheric particulate matter (PM) in rural field, rural village and urban areas of northern China,
594 *Environmental Pollution*, 185, 134-140, <https://doi.org/10.1016/j.envpol.2013.10.042>, 2014.
- 595 Li, X., Ye, C., Lu, K., Xue, C., Li, X., and Zhang, Y.: Accurately Predicting Spatiotemporal Variations of
596 Near-Surface Nitrous Acid (HONO) Based on a Deep Learning Approach, *Environmental Science &*
597 *Technology*, 58, 13035-13046, <https://doi.org/10.1021/acs.est.4c02221>, 2024a.
- 598 Li, Y., Qiao, L., Liu, M., Yang, Y., Yu, F., Yuan, X., Wang, Q., Ma, Q., and Zuo, J.: Access to affordable
599 and clean domestic heating: A critical review on rural clean heating transformation in China's Jing-Jin-
600 Ji and its surrounding areas, *Energy and Buildings*, 323, 114829,
601 <https://doi.org/10.1016/j.enbuild.2024.114829>, 2024b.
- 602 Liu, J., Weng, F., and Li, Z.: Satellite-based PM_{2.5} estimation directly from reflectance at the top of the
603 atmosphere using a machine learning algorithm, *Atmospheric Environment*, 208, 113-122,
604 <https://doi.org/10.1016/j.atmosenv.2019.04.002>, 2019.
- 605 Liu, R., Ma, Z., Gasparrini, A., de la Cruz, A., Bi, J., and Chen, K.: Integrating Augmented In Situ
606 Measurements and a Spatiotemporal Machine Learning Model To Back Extrapolate Historical Particulate
607 Matter Pollution over the United Kingdom: 1980–2019, *Environmental Science & Technology*, 57,
608 21605-21615, <https://doi.org/10.1021/acs.est.3c05424>, 2023.
- 609 Lundberg, S. M. and Lee, S.-I.: A unified approach to interpreting model predictions, *Proceedings of the*
610 *31st International Conference on Neural Information Processing Systems*, Long Beach, California,
611 USA2017.
- 612 Ministry of Ecology and Environment of the People's Republic of China: Ambient air quality standards,
613 <https://www.mee.gov.cn/ywgz/fgbz/bz/bzwb/dqhjbh/dqhjlzlbz/201203/W020120410330232398521.pdf>,
614 last access: 22 October 2024, 2012.
- 615 Ministry of Ecology and Environment of the People's Republic of China: Report on the state of the
616 ecology and environment in China,
617 <http://english.mee.gov.cn/Resources/Reports/soe/SOEE2017/201808/P020180801597738742758.pdf>,
618 last access: 22 October 2024, 2017.
- 619 Park, S., Shin, M., Im, J., Song, C. K., Choi, M., Kim, J., Lee, S., Park, R., Kim, J., Lee, D. W., and Kim,
620 S. K.: Estimation of ground-level particulate matter concentrations through the synergistic use of satellite



- 621 observations and process-based models over South Korea, *Atmos. Chem. Phys.*, 19, 1097-1113,
622 <https://doi.org/10.5194/acp-19-1097-2019>, 2019.
- 623 Park, S., Lee, J., Im, J., Song, C.-K., Choi, M., Kim, J., Lee, S., Park, R., Kim, S.-M., Yoon, J., Lee, D.-
624 W., and Quackenbush, L. J.: Estimation of spatially continuous daytime particulate matter concentrations
625 under all sky conditions through the synergistic use of satellite-based AOD and numerical models,
626 *Science of The Total Environment*, 713, 136516, <https://doi.org/10.1016/j.scitotenv.2020.136516>, 2020.
- 627 Qin, K., Han, X., Li, D., Xu, J., Loyola, D., Xue, Y., Zhou, X., Li, D., Zhang, K., and Yuan, L.: Satellite-
628 based estimation of surface NO₂ concentrations over east-central China: A comparison of POMINO and
629 OMNO_{2d} data, *Atmospheric Environment*, 224, 117322,
630 <https://doi.org/10.1016/j.atmosenv.2020.117322>, 2020.
- 631 Qiu, M., Zigler, C., and Selin, N. E.: Statistical and machine learning methods for evaluating trends in
632 air quality under changing meteorological conditions, *Atmos. Chem. Phys.*, 22, 10551-10566,
633 <https://doi.org/10.5194/acp-22-10551-2022>, 2022.
- 634 Rodriguez, J. D., Perez, A., and Lozano, J. A.: Sensitivity Analysis of k-Fold Cross Validation in
635 Prediction Error Estimation, *IEEE Transactions on Pattern Analysis and Machine Intelligence*, 32, 569-
636 575, <https://doi.org/10.1109/TPAMI.2009.187>, 2010.
- 637 Shen, G., Ru, M., Du, W., Zhu, X., Zhong, Q., Chen, Y., Shen, H., Yun, X., Meng, W., Liu, J., Cheng, H.,
638 Hu, J., Guan, D., and Tao, S.: Impacts of air pollutants from rural Chinese households under the rapid
639 residential energy transition, *Nature Communications*, 10, 3405, 10.1038/s41467-019-11453-w, 2019.
- 640 Shi, S., Chen, R., Wang, P., Zhang, H., Kan, H., and Meng, X.: An Ensemble Machine Learning Model
641 to Enhance Extrapolation Ability of Predicting Coarse Particulate Matter with High Resolutions in China,
642 *Environmental Science & Technology*, 58, 19325-19337, <https://doi.org/10.1021/acs.est.4c08610>, 2024.
- 643 Sicard, P., Agathokleous, E., Anenberg, S. C., De Marco, A., Paoletti, E., and Calatayud, V.: Trends in
644 urban air pollution over the last two decades: A global perspective, *Science of The Total Environment*,
645 858, 160064, <https://doi.org/10.1016/j.scitotenv.2022.160064>, 2023.
- 646 Song, C., Liu, B., Cheng, K., Cole, M. A., Dai, Q., Elliott, R. J. R., and Shi, Z.: Attribution of Air Quality
647 Benefits to Clean Winter Heating Policies in China: Combining Machine Learning with Causal Inference,
648 *Environmental Science & Technology*, 57, 17707-17717, <https://doi.org/10.1021/acs.est.2c06800>, 2023.
- 649 Song, Z., Chen, B., and Huang, J.: Combining Himawari-8 AOD and deep forest model to obtain city-
650 level distribution of PM_{2.5} in China, *Environmental Pollution*, 297, 118826,
651 <https://doi.org/10.1016/j.envpol.2022.118826>, 2022a.
- 652 Song, Z., Zhao, L., Ye, Q., Ren, Y., Chen, R., and Chen, B.: The Reconstruction of FY-4A and FY-4B
653 Cloudless Top-of-Atmosphere Radiation and Full-Coverage Particulate Matter Products Reveals the
654 Influence of Meteorological Factors in Pollution Events, <https://doi.org/10.3390/rs16183363>, 2024.
- 655 Song, Z., Chen, B., Zhang, P., Guan, X., Wang, X., Ge, J., Hu, X., Zhang, X., and Wang, Y.: High temporal
656 and spatial resolution PM_{2.5} dataset acquisition and pollution assessment based on FY-4A TOAR data
657 and deep forest model in China, *Atmospheric Research*, 274, 106199,
658 <https://doi.org/10.1016/j.atmosres.2022.106199>, 2022b.
- 659 Southerland, V. A., Brauer, M., Mohegh, A., Hammer, M. S., van Donkelaar, A., Martin, R. V., Apte, J.
660 S., and Anenberg, S. C.: Global urban temporal trends in fine particulate matter (PM_{2.5}) and attributable
661 health burdens: estimates from global datasets, *The Lancet Planetary Health*, 6, e139-e146,
662 [https://doi.org/10.1016/S2542-5196\(21\)00350-8](https://doi.org/10.1016/S2542-5196(21)00350-8), 2022.
- 663 State Council of the People's Republic of China: Action Plan on Air Pollution Prevention and Control,
664 http://www.gov.cn/zwqk/2013-09/12/content_2486773.htm, last access: 22 October 2024, 2013.



- 665 State Council of the People's Republic of China: Assessment Method of Air Pollution Prevention and
666 Control Action Plan, http://www.gov.cn/zhengce/content/2014-05/27/content_8830.htm, last access:
667 22 October 2024, 2014.
- 668 Vu, T. V., Shi, Z., Cheng, J., Zhang, Q., He, K., Wang, S., and Harrison, R. M.: Assessing the impact of
669 clean air action on air quality trends in Beijing using a machine learning technique, *Atmos. Chem. Phys.*,
670 19, 11303–11314, <https://doi.org/10.5194/acp-19-11303-2019>, 2019.
- 671 Wang, B., Yuan, Q., Yang, Q., Zhu, L., Li, T., and Zhang, L.: Estimate hourly PM_{2.5} concentrations from
672 Himawari-8 TOA reflectance directly using geo-intelligent long short-term memory network,
673 *Environmental Pollution*, 271, 116327, <https://doi.org/10.1016/j.envpol.2020.116327>, 2021.
- 674 Wang, J., Lin, J., Liu, Y., Wu, F., Ni, R., Chen, L., Ren, F., Du, M., Li, Z., Zhang, H., and Liu, Z.: Direct
675 and indirect consumption activities drive distinct urban-rural inequalities in air pollution-related
676 mortality in China, *Science Bulletin*, 69, 544–553, <https://doi.org/10.1016/j.scib.2023.12.023>, 2024a.
- 677 Wang, R., Tao, S., Ciais, P., Shen, H. Z., Huang, Y., Chen, H., Shen, G. F., Wang, B., Li, W., Zhang, Y.
678 Y., Lu, Y., Zhu, D., Chen, Y. C., Liu, X. P., Wang, W. T., Wang, X. L., Liu, W. X., Li, B. G., and Piao, S.
679 L.: High-resolution mapping of combustion processes and implications for CO₂ emissions,
680 *Atmos. Chem. Phys.*, 13, 5189–5203, 10.5194/acp-13-5189-2013, 2013.
- 681 Wang, W., Zhao, C., Dong, C., Yu, H., Wang, Y., and Yang, X.: Is the key-treatment-in-key-areas
682 approach in air pollution control policy effective? Evidence from the action plan for air pollution
683 prevention and control in China, *Science of The Total Environment*, 843, 156850,
684 <https://doi.org/10.1016/j.scitotenv.2022.156850>, 2022a.
- 685 Wang, X., Wang, T., Xu, J., Shen, Z., Yang, Y., Chen, A., Wang, S., Liang, E., and Piao, S.: Enhanced
686 habitat loss of the Himalayan endemic flora driven by warming-forced upslope tree expansion, *Nature
687 Ecology & Evolution*, 6, 890–899, <https://doi.org/10.1038/s41559-022-01774-3>, 2022b.
- 688 Wang, Y., Hu, Y., Jiang, S., and Zhao, B.: Distinguishing urban-rural difference in Chinese population
689 exposure to ambient air pollutants, *Atmospheric Environment*, 334, 120704,
690 <https://doi.org/10.1016/j.atmosenv.2024.120704>, 2024b.
- 691 Wang, Y., Yu, H., Li, L., Li, J., Sun, J., Shi, J., and Li, J.: Long-term trend of dust event duration over
692 Northwest China, *Science of The Total Environment*, 951, 175819,
693 <https://doi.org/10.1016/j.scitotenv.2024.175819>, 2024c.
- 694 Wei, J., Huang, W., Li, Z., Xue, W., Peng, Y., Sun, L., and Cribb, M.: Estimating 1-km-resolution PM_{2.5}
695 concentrations across China using the space-time random forest approach, *Remote Sensing of
696 Environment*, 231, 111221, <https://doi.org/10.1016/j.rse.2019.111221>, 2019.
- 697 Wei, J., Li, Z., Lyapustin, A., Sun, L., Peng, Y., Xue, W., Su, T., and Cribb, M.: Reconstructing 1-km-
698 resolution high-quality PM_{2.5} data records from 2000 to 2018 in China: spatiotemporal variations and
699 policy implications, *Remote Sensing of Environment*, 252, 112136,
700 <https://doi.org/10.1016/j.rse.2020.112136>, 2021.
- 701 Wei, J., Li, Z., Cribb, M., Huang, W., Xue, W., Sun, L., Guo, J., Peng, Y., Li, J., Lyapustin, A., Liu, L.,
702 Wu, H., and Song, Y.: Improved 1 km resolution PM_{2.5} estimates across China using enhanced space-
703 time extremely randomized trees, *Atmos. Chem. Phys.*, 20, 3273–3289, <https://doi.org/10.5194/acp-20-3273-2020>, 2020.
- 705 West, J. J., Cohen, A., Dentener, F., Brunekreef, B., Zhu, T., Armstrong, B., Bell, M. L., Brauer, M.,
706 Carmichael, G., Costa, D. L., Dockery, D. W., Kleeman, M., Krzyzanowski, M., Künzli, N., Liousse, C.,
707 Lung, S.-C. C., Martin, R. V., Pöschl, U., Pope, C. A., III, Roberts, J. M., Russell, A. G., and Wiedinmyer,
708 C.: “What We Breathe Impacts Our Health: Improving Understanding of the Link between Air Pollution



- 709 and Health", Environmental Science & Technology, 50, 4895-4904,
710 <https://doi.org/10.1021/acs.est.5b03827>, 2016.
- 711 Xiao, Q., Zheng, Y., Geng, G., Chen, C., Huang, X., Che, H., Zhang, X., He, K., and Zhang, Q.:
712 Separating emission and meteorological contributions to long-term PM_{2.5} trends over eastern China
713 during 2000–2018, Atmos. Chem. Phys., 21, 9475-9496, <https://doi.org/10.5194/acp-21-9475-2021>,
714 2021.
- 715 Xue, T., Liu, J., Zhang, Q., Geng, G., Zheng, Y., Tong, D., Liu, Z., Guan, D., Bo, Y., Zhu, T., He, K., and
716 Hao, J.: Rapid improvement of PM_{2.5} pollution and associated health benefits in China during 2013–
717 2017, Science China Earth Sciences, 62, 1847-1856, <https://doi.org/10.1007/s11430-018-9348-2>, 2019.
- 718 Yang, J., Lin, Z., and Shi, S.: Household air pollution and attributable burden of disease in rural China:
719 A literature review and a modelling study, Journal of Hazardous Materials, 470, 134159,
720 <https://doi.org/10.1016/j.jhazmat.2024.134159>, 2024.
- 721 Yang, N., Shi, H., Tang, H., and Yang, X.: Geographical and temporal encoding for improving the
722 estimation of PM_{2.5} concentrations in China using end-to-end gradient boosting, Remote Sensing of
723 Environment, 269, 112828, <https://doi.org/10.1016/j.rse.2021.112828>, 2022.
- 724 Yang, Q., Kim, J., Cho, Y., Lee, W.-J., Lee, D.-W., Yuan, Q., Wang, F., Zhou, C., Zhang, X., Xiao, X.,
725 Guo, M., Guo, Y., Carmichael, G. R., and Gao, M.: A synchronized estimation of hourly surface
726 concentrations of six criteria air pollutants with GEMS data, npj Climate and Atmospheric Science, 6,
727 94, <https://doi.org/10.1038/s41612-023-00407-1>, 2023.
- 728 Yin, J., Mao, F., Zang, L., Chen, J., Lu, X., and Hong, J.: Retrieving PM_{2.5} with high spatio-temporal
729 coverage by TOA reflectance of Himawari-8, Atmospheric Pollution Research, 12, 14-20,
730 <https://doi.org/10.1016/j.apr.2021.02.007>, 2021.
- 731 Yin, P., Brauer, M., Cohen, A. J., Wang, H., Li, J., Burnett, R. T., Stanaway, J. D., Causey, K., Larson, S.,
732 Godwin, W., Frostad, J., Marks, A., Wang, L., Zhou, M., and Murray, C. J. L.: The effect of air pollution
733 on deaths, disease burden, and life expectancy across China and its provinces, 1990–2017: an analysis
734 for the Global Burden of Disease Study 2017, The Lancet Planetary Health, 4, e386-e398,
735 [https://doi.org/10.1016/S2542-5196\(20\)30161-3](https://doi.org/10.1016/S2542-5196(20)30161-3), 2020.
- 736 Yu, Y., Dai, C., Wei, Y., Ren, H., and Zhou, J.: Air pollution prevention and control action plan
737 substantially reduced PM_{2.5} concentration in China, Energy Economics, 113, 106206,
738 <https://doi.org/10.1016/j.eneco.2022.106206>, 2022.
- 739 Yun, X., Shen, G., Shen, H., Meng, W., Chen, Y., Xu, H., Ren, Y., Zhong, Q., Du, W., Ma, J., Cheng, H.,
740 Wang, X., Liu, J., Wang, X., Li, B., Hu, J., Wan, Y., and Tao, S.: Residential solid fuel emissions
741 contribute significantly to air pollution and associated health impacts in China, Science Advances, 6,
742 eaba7621, 10.1126/sciadv.aba7621, 2020.
- 743 Zhai, S., Jacob, D. J., Wang, X., Shen, L., Li, K., Zhang, Y., Gui, K., Zhao, T., and Liao, H.: Fine
744 particulate matter (PM_{2.5}) trends in China, 2013–2018: separating contributions from anthropogenic
745 emissions and meteorology, Atmos. Chem. Phys., 19, 11031-11041, <https://doi.org/10.5194/acp-19-11031-2019>, 2019.
- 746
747 Zhang, H., Di, B., Liu, D., Li, J., and Zhan, Y.: Spatiotemporal distributions of ambient SO₂ across China
748 based on satellite retrievals and ground observations: Substantial decrease in human exposure during
749 2013–2016, Environmental Research, 179, 108795, <https://doi.org/10.1016/j.envres.2019.108795>, 2019a.
- 750 Zhang, Q., He, K., and Huo, H.: Cleaning China's air, Nature, 484, 161-162,
751 <https://doi.org/10.1038/484161a>, 2012.
- 752 Zhang, Q., Shi, R., Singh, V. P., Xu, C.-Y., Yu, H., Fan, K., and Wu, Z.: Droughts across China: Drought



753 factors, prediction and impacts, *Science of The Total Environment*, 803, 150018,
754 <https://doi.org/10.1016/j.scitotenv.2021.150018>, 2022a.

755 Zhang, Q., Zheng, Y., Tong, D., Shao, M., Wang, S., Zhang, Y., Xu, X., Wang, J., He, H., Liu, W., Ding,
756 Y., Lei, Y., Li, J., Wang, Z., Zhang, X., Wang, Y., Cheng, J., Liu, Y., Shi, Q., Yan, L., Geng, G., Hong, C.,
757 Li, M., Liu, F., Zheng, B., Cao, J., Ding, A., Gao, J., Fu, Q., Huo, J., Liu, B., Liu, Z., Yang, F., He, K.,
758 and Hao, J.: Drivers of improved PM_{2.5} air quality in China from 2013 to 2017, *Proceedings of the*
759 *National Academy of Sciences*, 116, 24463-24469, <https://doi.org/10.1073/pnas.1907956116>, 2019b.

760 Zhang, X., Brandt, M., Tong, X., Ciais, P., Yue, Y., Xiao, X., Zhang, W., Wang, K., and Fensholt, R.: A
761 large but transient carbon sink from urbanization and rural depopulation in China, *Nature Sustainability*,
762 5, 321-328, <https://doi.org/10.1038/s41893-021-00843-y>, 2022b.

763 Zhao, B., Zheng, H., Wang, S., Smith, K. R., Lu, X., Aunan, K., Gu, Y., Wang, Y., Ding, D., Xing, J., Fu,
764 X., Yang, X., Liou, K.-N., and Hao, J.: Change in household fuels dominates the decrease in PM_{2.5}
765 exposure and premature mortality in China in 2005–2015, *Proceedings of the National Academy of*
766 *Sciences*, 115, 12401-12406, <https://doi.org/10.1073/pnas.1812955115>, 2018.

767 Zheng, B., Tong, D., Li, M., Liu, F., Hong, C., Geng, G., Li, H., Li, X., Peng, L., Qi, J., Yan, L., Zhang,
768 Y., Zhao, H., Zheng, Y., He, K., and Zhang, Q.: Trends in China's anthropogenic emissions since 2010 as
769 the consequence of clean air actions, *Atmos. Chem. Phys.*, 18, 14095-14111, [https://doi.org/10.5194/acp-](https://doi.org/10.5194/acp-18-14095-2018)
770 [18-14095-2018](https://doi.org/10.5194/acp-18-14095-2018), 2018.

771 Zheng, H., Kong, S., He, Y., Song, C., Cheng, Y., Yao, L., Chen, N., and Zhu, B.: Enhanced ozone
772 pollution in the summer of 2022 in China: The roles of meteorology and emission variations,
773 *Atmospheric Environment*, 301, 119701, <https://doi.org/10.1016/j.atmosenv.2023.119701>, 2023.

774 Zhong, Q., Ma, J., Shen, G., Shen, H., Zhu, X., Yun, X., Meng, W., Cheng, H., Liu, J., Li, B., Wang, X.,
775 Zeng, E. Y., Guan, D., and Tao, S.: Distinguishing Emission-Associated Ambient Air PM_{2.5}
776 Concentrations and Meteorological Factor-Induced Fluctuations, *Environmental Science & Technology*,
777 52, 10416-10425, <https://doi.org/10.1021/acs.est.8b02685>, 2018.

778 Zhong, Q., Tao, S., Ma, J., Liu, J., Shen, H., Shen, G., Guan, D., Yun, X., Meng, W., Yu, X., Cheng, H.,
779 Zhu, D., Wan, Y., and Hu, J.: PM_{2.5} reductions in Chinese cities from 2013 to 2019 remain significant
780 despite the inflating effects of meteorological conditions, *One Earth*, 4, 448-458,
781 <https://doi.org/10.1016/j.oneear.2021.02.003>, 2021.

782